

Suppression of ferromagnetic ordering in doped manganites: Effects of the superexchange interaction

Hongsuk Yi

Center for CMR Materials, Korea Research Institute of Standards and Science,
Yusong, P.O. Box 102, Taejon 305-600, Korea

Jaejun Yu

Department of Physics and Center for Strongly Correlated Materials Research,
Seoul National University, Seoul 151-742, Korea

Sung-Ik Lee

National Creative Research Initiative Center for Superconductivity,
Pohang University of Science and Technology, Pohang 790-784, Korea
(today)

From a Monte Carlo study of the ferromagnetic Kondo lattice model for doped manganites, including the antiferromagnetic superexchange interaction (J_{AF}), we found that the ferromagnetic ordering was suppressed as J_{AF} increased. The ferromagnetic transition temperature T_c , as obtained from a mean field fit to the calculated susceptibilities, was found to decrease monotonically with increasing J_{AF} . Further, the suppression in T_c scales with the bandwidth narrowing induced by the antiferromagnetic frustration originating from J_{AF} . From these results, we propose that the change in the superexchange interaction strength between the t_{2g} electrons of the Mn ions is one of the mechanisms responsible for the suppression in T_c observed in manganites of the type $(La_{0.7-y}Pr_y)Ca_{0.3}MnO_3$.

PACS numbers: 75.30.-m, 75.30.et, 71.10.-w

I. INTRODUCTION

Since the discovery of colossal magnetoresistance (CMR) in the doped manganites, $Ln_{1-x}A_xMnO_3$ (Ln =trivalent lanthanide, A =divalent alkaline), great efforts have been made to understand the metal-insulator and/or ferro-to-antiferromagnetic transitions driven by the substitution of cations with different sizes, such as $(La_{0.7-y}Pr_y)Ca_{0.3}MnO_3$.¹⁻³ For the $La_{0.7}Ca_{0.3}MnO_3$ system, i.e., $y=0$, which corresponds to a hole doping of $x \sim 1/3$, a sharp resistivity peak is observed near the transition temperature $T_c \approx 260$ K. While the compound is insulating and paramagnetic above T_c , it becomes a metallic ferromagnet below T_c . The double exchange (DE) model⁴ has been widely used to describe the nature of the metallic and the ferromagnetic (FM) states in a small range of doping concentrations near $x \sim 1/3$. However, it was claimed that other effects such as the Jahn-Teller (JT) distortion,^{5,6} the orbital degeneracy,^{7,8} and the antiferromagnetic (AF) superexchange interaction (J_{AF})⁹⁻¹¹ should be included for a more accurate description over a wide range of x values ($0 \lesssim x \lesssim 1$).

Recent experiments¹⁻³ on $La_{2/3}A_{1/3}MnO_3$ showed that the substitution of trivalent ions such as Y, Pr, and Dy at the La^{3+} sites having a smaller average radius, $\langle R_o \rangle$, for the lanthanide led to the modification of the Mn-O-Mn bond angle (Θ) and the Mn-O bond length. Those experiments also revealed that these effects caused a decrease in T_c and a reduction in the magnetization below T_c , as well as an increase in the CMR effects near T_c . In general, the narrowing of the electronic bandwidth is

considered to be the origin of the T_c suppression effects. In this regard, Millis *et al.*⁵ and Rodriguez-Martinez and Attfield⁶ suggested that the electron-phonon coupling arising from the dynamic JT distortion due to the varying $\langle R_o \rangle$ could induce the bandwidth narrowing and suppress T_c rapidly. However, it was suggested that mechanisms other than the electron-phonon coupling could also explain the same behavior.¹⁻³ In particular, Radaelli *et al.*² observed that the suppression of T_c was more sensitive to the bandwidth narrowing due to the change in Θ rather than to the electron-phonon coupling. The change in the bond angle will not only influence the DE hopping integral (t_σ^{DE}) between $e_g(\text{Mn})-2p_\sigma(\text{O})-e_g(\text{Mn})$ orbitals of a FM nature but also affect the superexchange hopping integral (t_π^{AF}) through a hybridization of the $t_{2g}(\text{Mn})-2p_\pi(\text{O})-t_{2g}(\text{Mn})$ orbitals of an AF nature.³ Thus, it is expected that both the double exchange and the superexchange terms will compete with each other and play a significant role when structural distortions occur. Therefore, it would be of great interest to study the role of J_{AF} in the doped perovskite Mn-oxides.

In this paper, we present results of our Monte Carlo calculations for the FM Kondo lattice model which was modified by introducing the J_{AF} . From the calculations of the spin correlations, we found that the ordered FM state changes into an incommensurate (IC) state due to the magnetic fluctuations induced by the increase of J_{AF} . It was also shown from the obtained susceptibilities that the mean-field T_c monotonically decreased with J_{AF} . From the density-of-states calculations, we were able to determine that the bandwidth narrowing induced

by the AF frustration originating from J_{AF} scaled with the reduction of T_c . This behavior is consistent with that seen during recent experimental observations of the $\text{La}_{2/3-y}\text{Pr}_y\text{Ca}_{1/3}\text{MnO}_3$ system.

II. MODEL HAMILTONIAN AND CALCULATION METHOD

The model Hamiltonian studied in this paper can be written as a sum of three terms:

$$H = - \sum_{\langle ij \rangle, \sigma}^L \left(t_{ij} c_{i\sigma}^+ c_{j\sigma} + \text{H.c.} \right) - J_H \sum_{i,ab}^L \vec{S}_i \cdot \vec{\sigma}_{ab} c_{ia}^+ c_{ib} + J_{AF} \sum_{i,j}^L \vec{S}_i \cdot \vec{S}_j, \quad (1)$$

where the \vec{S}_i represents the localized spin of the t_{2g} electrons at the site \vec{R}_i , the $c_{i\sigma}$ is a destruction operator for one species of e_g fermions. The t_{ij} is the nearest-neighbor hopping amplitude for the e_g electrons, and $J_H > 0$ is the FM Hund's rule coupling between the e_g conduction electrons and the t_{2g} localized electrons. The last term represents the AF superexchange interaction between the t_{2g} electrons of neighboring Mn sites. In our calculation, we treat the localized t_{2g} spin \vec{S}_i as a classical spin; $\vec{S}_i = 3/2(\sin \theta_i \cos \phi_i \hat{x} + \sin \theta_i \sin \phi_i \hat{y} + \cos \theta_i \hat{z})$. Within this approximation, the trace over the e_g electrons in the partition function can be carried out exactly since Eq. (1) is quadratic in the fermionic field. The integration over the localized spins $\{\theta_i, \phi_i\}$ is performed using a standard Metropolis algorithm.^{9,10} In our calculation, unless stated otherwise, we take $t = 1$ as the unit of energy, $J_H = 8t$, the temperature $T = 0.01t$, and $L = 6 \times 6$ with a periodic boundary condition (PBC). Because the J_{AF} is estimated^{7,11} to be on the order of $J_{AF} \lesssim 0.01$ eV while typical values for t and J_H are ~ 0.1 eV and 1 eV, respectively. The range of values for J_H considered in this work looks reasonable in comparison with those seen in experiments.

III. RESULTS

A. Effects of J_{AF} in spin-spin correlation

For a given chemical potential $\mu = -7.4$, the electron density $\langle n \rangle$ ($= 1 - x$) was determined as a result of simulations. In Fig. 1(a), $\langle n \rangle$ is plotted as a function of J_{AF} . While $\langle n \rangle$ stays almost constant for the range of $J_{AF} \lesssim 0.11$, an abrupt jump is observed in $\langle n \rangle$ near $J_{AF} \approx 0.115$. For small J_{AF} , the average density is about 0.65, approximately $x \sim 1/3$, which is almost independent of J_{AF} . In this work, we focus on the system with $x \approx 1/3$ because the FM metallic phase with large CMR

effects is observed in $\text{La}_{1-x}\text{A}_x\text{MnO}_3$ with $x \approx 1/3$ and because dramatic FM-AF and metal-insulator transitions occur when La ions are replaced by Pr. With increasing J_{AF} , the system runs into a phase separation (PS) region where both AF and IC phases coexist. It should be noted that the phase separation induced by J_{AF} is similar to the discontinuity observed in the density as a function of μ .^{9,10}

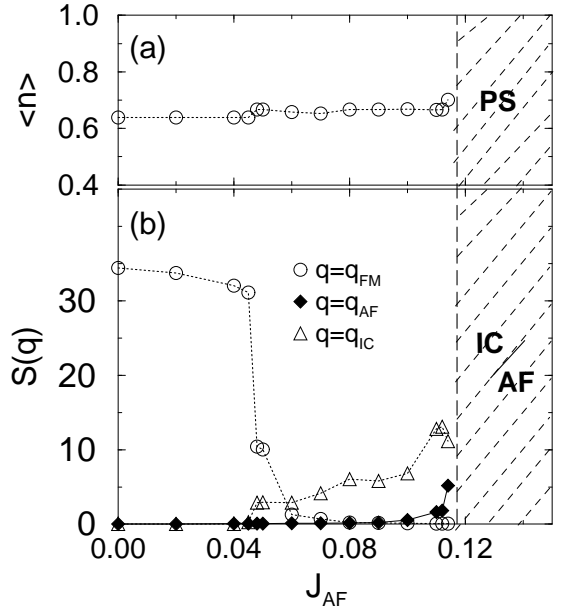


FIG. 1. (a) The carrier density vs the antiferromagnetic superexchange interaction J_{AF} on a 6×6 lattice with $J_H = 8t$, $T = t/100$, and $\mu = -7.4$. The notation PS means phase separation. (b) Peak intensities $S(\mathbf{q})$ for $\mathbf{q}_{FM} = (0, 0)$, $\mathbf{q}_{IC} = (\alpha\pi, \pi)$ ($0 < \alpha < 1$) and $\mathbf{q}_{AF} = (\pi, \pi)$ as a function of doping J_{AF} .

The spin structure factor $S(\mathbf{q})$ given by the Fourier transform of the spin-spin correlation function, $S(\mathbf{q}) \equiv \sum_{i,1} e^{i\mathbf{q} \cdot \mathbf{r}} \langle \vec{S}_i \cdot \vec{S}_{i+1} \rangle$, was also evaluated as a function of J_{AF} and is plotted in Fig. 1(b). The different \mathbf{q} values of $(0, 0)$, $(\alpha\pi, \pi)$ with $(0 < \alpha < 1)$, and (π, π) correspond to the FM, IC and AF phases, respectively. The FM fluctuation is dominant for $J_{AF} < 0.045$ and is drastically reduced for $J_{AF} \gtrsim 0.05$, where the IC component starts to develop. Strong IC spin correlations become significantly pronounced with a further increase of J_{AF} . The presence of IC state arising from the frustration of AF insulating state has been pointed out to play an important role in the transport properties in manganites.¹² Also, near $J_{AF} \approx 0.115$, a small region of J_{AF} exists where the IC and the AF fluctuations are competing. Due to the PS effect mentioned above, the two phases should segregate, leading to the IC and the AF phases. However, to understand the fine details of the magnetic properties, the one-orbital model is not sufficient due to the highly anisotropic nature of the orbital degree of freedom in undoped manganites. Certainly a two orbital

model is needed to describe the non-trivial interplay between the spin and orbital ordering in insulating phase of LaMnO_3 .⁸

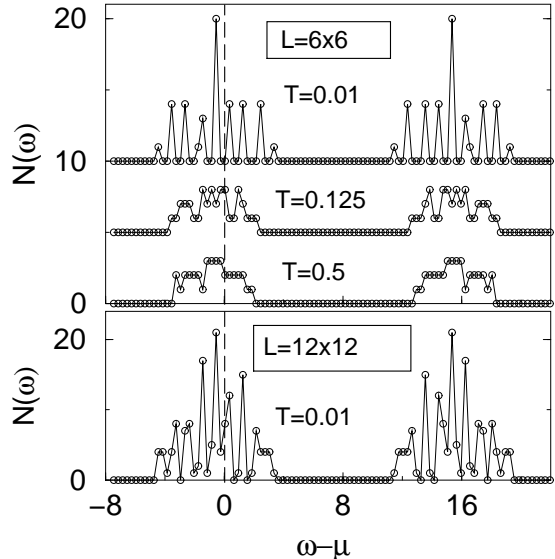


FIG. 2. Density-of-states $N(\omega)$ as a function of $\epsilon - \mu$ at three different temperatures with $J_{AF} = 0.0$ at $x \approx 1/3$ with a PBC. In the lower panel, the result for a larger system size of $L = 12 \times 12$ is shown.

B. Bandwidth narrowing

As shown in Fig. 2, we calculated the density-of-states $N(\omega)$, from the eigenvalues of the Hamiltonian in Eq. (1) for many configurations at three different temperatures and system sizes with $J_{AF} = 0.0$. The broken line at $\omega - \mu = 0$ indicates the Fermi energy E_F .¹³ It can be seen that the bands are split into two major parts with the separation between the lower and the upper bands corresponding to the energy splitting $2J_H$ by the Hund coupling. In the low-temperature limit ($T = 0.01$), the spiky shape of each band is due to the finite-size effect, as shown by the calculations for two system sizes, $L = 6 \times 6$ in the upper panel and 12×12 in the lower panel. As the temperature increases, this shape is smeared out, and at the same time the width of each band is reduced due to the disorder of the local t_{2g} spins. The system is FM metallic since the density-of-states at E_F remains finite.

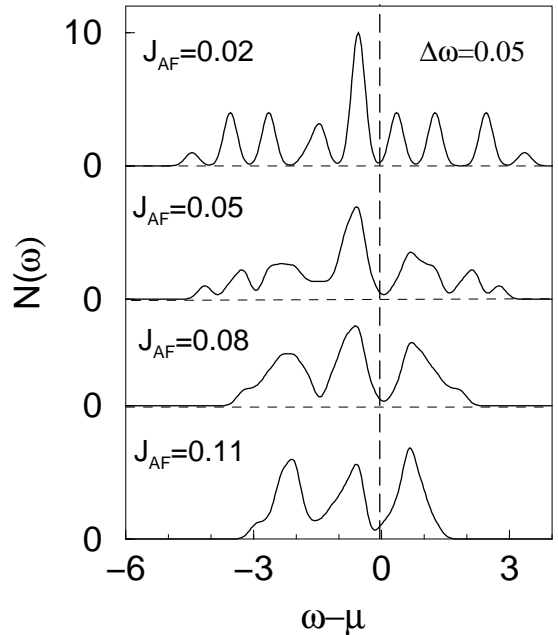


FIG. 3. Density-of-states as a function of $\epsilon - \mu$ for $J_{AF} = 0.02, 0.05, 0.08$ and 0.11 .

The $N(\omega)$ of the lower band is shown for various values of J_{AF} in Fig. 3. These curves are smoothed out with a Gaussian broadening of $\Delta\omega = 0.05$. This broad spectrum of $N(\omega)$ is also observed for $0 \lesssim J_{AF} \lesssim 0.04$, which corresponds to the FM region in Fig. 1(b). With further increase in J_{AF} , we find that a significant difference exists in the nature of each band between the FM and the IC states. For $0.05 \lesssim J_{AF} \lesssim 0.11$, together with a strong band narrowing, the wide distribution of eigenvalues merge into three peaks while the E_F lies at the dip of $N(\omega)$.

In Fig. 4, the bandwidth determined from the density-of-states is plotted as a function of J_{AF} . We define the bandwidth of the lower band as $\Delta W \equiv \langle \epsilon_{max} - \epsilon_{min} \rangle$ where ϵ_{max} and ϵ_{min} are the maximum and the minimum energies of each band in Fig. 2. Surprisingly, the bandwidth has a unique dependence on J_{AF} in each magnetic region, as discussed above. In the metallic FM region, the bandwidth is independent of J_{AF} and is equal to about 8. This value is close to the one from the dispersion relation in the 2-dimensional DE model. The most dramatic change of W with J_{AF} is found in the metallic IC region. W monotonically decreases by half as J_{AF} increases from 0.04 to 0.11. The evolution of the bandwidth depicted in Fig. 4 is of great importance since the suppression of T_c in the doped manganites is closely related to the bandwidth narrowing. It implies that the AF frustration arising from J_{AF} can be an another candidate for the band narrowing mechanism in the doped manganite systems besides the JT-polaron effects⁵ and the random potentials due to the disorder of the cations.⁶

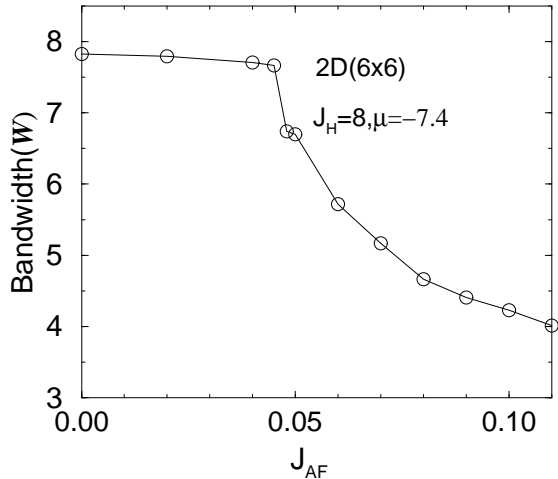


FIG. 4. Bandwidth as a function of J_{AF} for $J_H = 8$ and $T = 0.01$ with a PBC.

C. Suppression of ferromagnetic ordering

The temperature-dependent magnetic susceptibility is calculated from $\chi(T) \equiv \langle S_z^2 \rangle / k_B T$.¹¹ In Fig. 5, the inverse $\chi(T)$ is plotted vs temperature for various values of J_{AF} ; a Curie-Weiss behavior is seen for $\chi(T)$ at high temperatures. The mean-field transition temperature T_M is estimated by extrapolating the high-temperature data to the low-temperature limit. It is found that T_M decreases from positive to negative values, indicating a change of the interaction nature from FM to AF, with increasing J_{AF} . The change of T_M with J_{AF} implies that the magnetic interaction via the DE hopping mechanism is weakened by increasing the J_{AF} interaction.

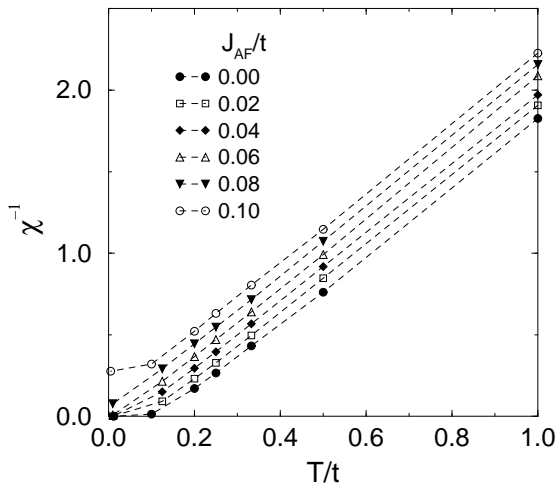


FIG. 5. Inverse susceptibility vs temperature for various values of J_{AF} with $J_H = 8t$, $T = t/100$, and $\mu = -7.4$.

Based on the estimated results of T_M in Fig. 5, the mean-field temperature vs J_{AF} phase diagram is shown in Fig. 6. T_M in the FM region is determined for two boundary conditions; a PBC (circles) and open boundary

condition (OBC) (squares). The AF region (triangles) is determined using only a PBC. The ferromagnetic T_M decreases linearly within the error limit, with increasing J_{AF} and reaches zero at $J_{AF} \approx 0.08$ above which the AF T_M start to develop. The inset shows an experimentally proposed phase diagram¹ for $\text{La}_{0.7-y}\text{Pr}_y\text{Ca}_{0.3}\text{MnO}_3$ as a function of Pr doping. A decrease in T_c when Pr doping increases implies a weaker DE hopping overlapping and a narrower bandwidth. The two phase diagrams shown in Fig. 6 exhibit a similarity between the Pr doping level and J_{AF} . As pointed out earlier, the substitution of Pr at La sites causes a smaller $\langle R_o \rangle$ and a smaller bond angle Θ , and the change in Θ modifies both the t_{σ}^{DE} due to the nature of $d\sigma$ hybridization and the t_{π}^{AF} due to $d\pi$ -type hybridization. However, while t is more sensitive to a change of bond angle Θ due to the nature of $d\sigma$ hybridization, the superexchange term J_{AF} , which relies on a $d\pi$ -type hybridization between $t_{2g}(\text{Mn})-p_{\pi}(\text{O})-t_{2g}(\text{Mn})$, is relatively insensitive to a change in the bond angle. Thus, an increase in J_{AF} , relative to the DE hopping integral t , is expected when Θ decreases. This behavior is consistent with the experimental evidence³ seen in the reduction of the magnetization with $\langle R_o \rangle$.

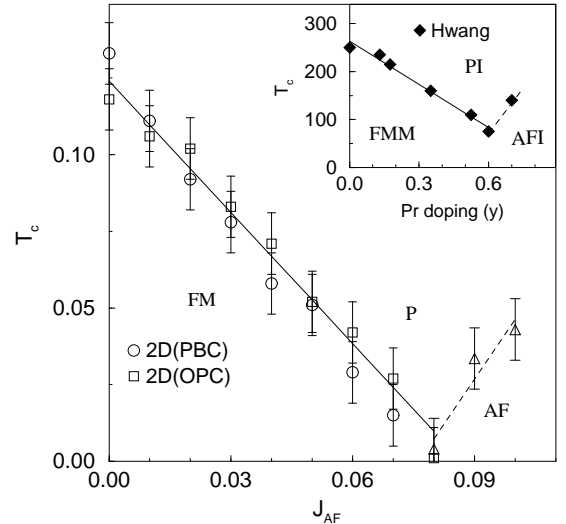


FIG. 6. Phase diagram of the 2D FM Kondo lattice model with $J_H = 8t$, as obtained by measuring the inverse susceptibilities at $x \sim 1/3$. The circles (squares) and triangles represent the phase boundaries between the paramagnetic (P) and the FM phases with a PBC (OBC) and between the P and the AF phases with a PBC respectively. The solid and the dash lines are guides for the eyes.

Indeed, when the bandwidth in Fig. 4 is compared with T_c in Fig. 6, the suppression in T_c for $\text{La}_{0.7-y}\text{Pr}_y\text{Ca}_{0.3}\text{MnO}_3$ correlates well, at least qualitatively, with the narrowing of the bandwidth. Further, the absence of internal spin structure, i.e., IC ordering, in Fig. 6 for $J_{AF} \lesssim 0.08$ is due to the mean-field approximation in determining T_M for χ . Thus, the bandwidth

narrowing in the metallic IC state is thought to be responsible for the observed T_c reduction. Consequently, in addition to the electron-phonon interactions arising from Jahn-Tell distortion, the magnetic frustration arising from the enhancement of J_{AF} should be considered as a cause of the bandwidth narrowing leading to the suppression in T_c . Here, it is noted that the effect of orbital degeneracy is not taken into account in this work. Since, however, many optimally doped metallic systems near $x \approx 0.3$ are pseudo-cubic in structure, the conduction electron hopping can be considered to be isotropic. On the other hand, the non-trivial interplay between spin and orbital degree of freedom in connection with orbital degeneracy has been pointed out to play an important role in the spin and orbital ordering in the undoped insulating phase of LaMnO_3 .⁷

IV. CONCLUSION

In conclusion, it is suggested that the superexchange interaction in the modified FM Kondo lattice model is one of the mechanisms responsible for the observed T_c reduction in $\text{La}_{0.7-y}\text{Pr}_y\text{Ca}_{0.3}\text{MnO}_3$. With a change in J_{AF} , magnetic frustration is induced and leads to a more complicated magnetic phase diagram. The bandwidth narrowing occurs for $0.05 \lesssim J_{AF} \lesssim 0.11$ in the metallic IC state and is thought to be responsible for the T_c reduction in $\text{La}_{0.7-y}\text{Pr}_y\text{Ca}_{0.3}\text{MnO}_3$. With our model, we found that bandwidth narrowing, accompanied by T_c reduction, can be induced by J_{AF} without electron-phonon coupling.

ACKNOWLEDGMENTS

This work was supported by Creative Research Initiatives of the Korean Ministry of Science and Technology. Additional support was provided by the Korea Science Engineering Foundation (95-0702-03-01-3). Part of the calculation was also performed on the JRCAT Supercomputer System, which is supported by New Energy and Industrial Technology Development Organization (NEDO) of Japan.

L. García-Muñoz, and X. Obradors, Phys. Rev. Lett. **76**, 1122 (1996).

⁴ C. Zener, Phys. Rev. **82**, 403 (1951); J. B. Goodenough, Phys. Rev. **100**, 565 (1955); P. W. Anderson and H. Hasegawa, Phys. Rev. **100**, 675 (1955); K. Kubo and N. Ohata, J. Phys. Soc. Jpn. **33**, 21 (1972).

⁵ A. J. Millis, P. B. Littlewood, and B. I. Shraiman, Phys. Rev. Lett. **74**, 5144 (1995); A. J. Millis, B. I. Shraiman, and R. Mueller, Phys. Rev. Lett. **77**, 175 (1996).

⁶ L. M. Rodriguez-Martinez and J. P. Attfield, Phys. Rev. B **54**, R15 622 (1996).

⁷ S. Ishihara, J. Inoue, and S. Maekawa, Phys. Rev. B **55**, 8280 (1997); R. Maezono, S. Ishihara, and N. Nagaosa, Phys. Rev. B **57**, R13 993 (1998).

⁸ W. Koshiba, Y. Kawamura, S. Ishihara, S. Okamoto, J. Inoue, and S. Maekawa, J. Phys. Soc. Jpn. **66**, 957 (1997).

⁹ S. Yunoki and A. Moreo, Phys. Rev. B **58**, 6403 (1998); S. Yunoki, J. Hu, A. Malvezzi, A. Moreo, N. Furukawa, and E. Dagotto, Phys. Rev. Lett. **80**, 845 (1998).

¹⁰ H. Yi and J. Yu, Phys. Rev. B **58**, 11 123 (1998); H. Yi and S. Lee, Phys. Rev. B **60**, 6250 (1999); H. Yi, J. Yu, and S. Lee, Eur. Phys. J. B **7**, 509 (1999).

¹¹ P. Horsch, J. Jaklic, and F. Mack, Phys. Rev. B **59**, R14 149 (1999).

¹² J. Inoue, and S. Maekawa, Phys. Rev. Lett. **74**, 3407 (1995).

¹³ The finite energy interval used for the density-of-states calculation is $\omega_0 = 0.3$.

¹ H. Y. Hwang, S-W. Cheong, P. G. Radaelli, M. Marezio, and B. Batlogg, Phys. Rev. Lett. **75**, 914 (1995).

² P. G. Radaelli, G. Iannone, M. Marezio, H. Y. Hwang, S-W. Cheong, J. D. Jorgensen, and D. N. Argyriou, Phys. Rev. B **56**, 8265 (1997).

³ J. L. García-Muñoz, J. Fontcuberta, B. Martínez, A. Seffar, S. Piñol, and X. Obradors, Phys. Rev. B **55**, R668 (1997); J. Fontcuberta, B. Martínez, A. Seffar, S. Piñol, J.